not possible. Similar characteristics were observed with somewhat larger bubbles of 5·5 mm initial equivalent diameter, where the asymptotic final velocity was somewhat higher (14·5 cm/s). It is noteworthy that condensation was not complete in any of the runs discussed. The maximum amount of vapor in the final stages is estimated at about ten per cent (weight) of the original vapor in the bubble. We have also noted that whereas the collapse time was rather consistent in the small bubbles (about 0·08 s after release) that of the larger size bubbles was more erratic, varying between 0·07 and 0·12 s after release. This non-uniform behavior of the larger bubbles is most probably associated with the greater variety of bubble shapes due to larger deformations of the larger bubbles.

The results obtained indicated that smoother velocity curves with less abrupt velocity changes would be obtained with larger bubbles under similar temperature driving forces. This observation is partly substantiated by the data obtained during the complementary study of single pentane drops evaporating in water which was at some temperature above the pentane normal boiling point. There the velocity increased gradually with vapor content [6]. One of these curves obtained for drops with initial diameter of about 2 mm is included in Fig. 1. The asymptotic constant velocity corresponding to that of the fully evaporated droplet (final diameter about 12 mm) was approximately 25 cm/s (not shown here). Generally the deviation between integrated, or average velocities, and differential point velocities seemed to decrease with increasing bubble diameter. This is consistent with the results obtained by Calderbank and Lochiel in their absorption studies. It is evident, however, that where asymptotic final values are reached, averaging the velocities over an arbitrary pool height or using the asymptotic value would be quite erroneous. For instance, using the asymptotic velocity as the representative value would introduce an error of about sixty per cent with respect to the velocity averaged over the condensation height corresponding to Fig. 1.

It is also interesting to note that no apparent effect of the temperature driving force on the velocity was noted in the condensation study where rather small temperature differences (up to 3·5 degC) were used. However, the velocity, averaged over the height required for complete evaporation, was found to decrease slightly with increase of the temperature gradient (up to 15 degC) with the 2 mm liquid drops (initial diameter) evaporating in sea water [6]. No effect of temperature on the velocity was noted with evaporation of larger drops with final bubble diameter of about 22 mm.

REFERENCES

1. P. H. CALDERBANK and A. C. LOCHIEL, *Chem. Engng Sci.* **19**, 485 (1964).
2. W. L. HABERMAN and R. K. MORTON, *Trans. Amer. Soc. Civil Engrs* **121**, 227 (1956).
3. J. H. LEONARD, Ph.D. Thesis, University of Pittsburg (1961). (From reference 1.)
4. S. UNO and R. C. KINTNER, *J. Amer. Inst. Chem. Engrs* **2**, 420 (1956).
5. S. SIDEMAN and G. HIRSCH, *A.I.Ch.E.Jl.* To be published.
6. S. SIDEMAN and Y. TAITEL, *Int. J. Heat Mass Transfer* **7**, 1273–1289 (1964).

Int. J. Heat Mass Transfer. Vol. 8, pp. 1172–1175. Pergamon Press 1965. Printed in Great Britain

DIFFUSION FROM A LINE SOURCE IN A TURBULENT BOUNDARY LAYER: COMPARISON OF THEORY AND EXPERIMENT

S. V. PATANKAR and R. G. TAYLOR
Mechanical Engineering Department, Imperial College, London

(*Received* 17 *February* 1965)

NOMENCLATURE*

a, b, constants in the velocity profile law;
c, concentration of the diffusing matter;
C_{max}, maximum value of concentration; concentration at the wall;
C_G, concentration in the main stream;
c_f, local drag coefficient;
G, flux of the diffusing matter per unit time and per unit length of the line source;
N_{Sc}, laminar Schmidt number;
$N_{Sc,\,t}$, turbulent Schmidt number;
U_{amb}, velocity of the ambient air stream;
u^+, non-dimensional velocity;
X', distance downstream from the origin of turbulent boundary layer;
X_0', distance of the line source from the origin of turbulent boundary layer;
x, distance downstream from the source;
x^+, non-dimensional distance along a stream line;
y, distance from and normal to the wall;

* Nomenclature as in [1] and [2].

y^+, non-dimensional distance from and normal to the wall;
δ, thickness of the velocity boundary layer;
$\epsilon_u{}^+$, non-dimensional total viscosity;
λ, distance from the wall at which $(c/C_{max}) = 0{\cdot}5$;
λ^+, non-dimensional form of λ;
μ, dynamic viscosity;
ν, kinematic viscosity;
ρ, density;
ϕ, turbulent contribution to $\epsilon_u{}^+$.

1. INTRODUCTION

In a recent paper [1] Poreh and Cermak report the results of an experimental investigation of the diffusion of ammonia gas from a line source into a two-dimensional turbulent boundary layer. The investigation reveals two distinct regions of similarity, namely the intermediate zone and the final zone, in which the concentration boundary layer shows respectively a developing and a fully developed character. Quantities measured in the intermediate zone, in which the concentration boundary layer is much thinner than the velocity boundary layer, are, at various positions downsteam: the concentration profiles; the concentration at the wall; and the distance λ from the wall at which the concentration is half the wall concentration.

In the appendix of a paper by Spalding [2], an exact analytical solution is presented for the problem of diffusion of heat from a line source into a two-dimensional turbulent boundary layer, the solution being valid whenever the thermal boundary layer is appreciably thinner than the velocity boundary layer.

The purpose of the present communication is to show that the equations and results of [2] give predictions of the experimental results of Poreh and Cermak [1] *in the intermediate zone*, and that the agreement between the theory and experiment is good.

2. THE PROBLEM OF DIFFUSION FROM A LINE SOURCE

The problem considered in [2] is the solution of the differential equation*:

$$\frac{\partial c}{\partial (x^+/N_{Sc,\,t})} = \frac{1}{u^+(1+\phi)} \frac{\partial}{\partial u^+}\left(\frac{(N_{Sc,\,t}/N_{Sc}) + \phi}{1+\phi} \frac{\partial c}{\partial u^+}\right)$$

with the boundary conditions:

$$\left.\begin{aligned} &x^+ = 0,\ u^+ > 0 \\ &\text{all } x^+,\ u^+ \to \infty \end{aligned}\right\} \quad : \quad c = C_G$$

$$x^+ > 0,\ u^+ = 0 \quad : \quad (\partial c/\partial u^+) = 0$$

$$x^+ > 0 \quad : \quad \int_0^\infty (c - C_G) u^+ \epsilon_u{}^+ \, du^+ = G\rho/\mu.$$

The solution presented in the appendix of [2] is based on the assumption $N_{Sc} = N_{Sc,\,t}$, on a power-law velocity profile of the form $y^+ = a(u^+)^b$, and the corresponding total viscosity profile $\epsilon_u{}^+ = ab(u^+)^{b-1}$.

If we regard the mass-transfer rate as too small to modify the velocity profile, the results of the solution in [2] lead to the following equations:

Concentration profile

$$\frac{c}{C_{max}} = \exp\left[-(\ln 2)(y/\lambda)^{(b+2)/b}\right] \tag{2.1}$$

(This is the modified form of equation (A.28) in [2]).

Concentration at the wall

$$\frac{C_{max}\mu}{G\rho} = \frac{(b+1)}{(b+2)^2}\left[\frac{(b+2)^2}{ab}\right]^{1/(b+2)}\left[\Gamma\left(\frac{2b+3}{b+2}\right)\right]^{-1}\left(\frac{N_{Sc,\,t}}{x^+}\right)^{(b+1)/(b+2)} \tag{2.2}$$

(This is obtained from equation (A.31) in [2] by putting $C_G = 0$, which is the appropriate boundary condition when the concentration boundary layer is thinner than the velocity boundary layer.)

Distance, λ, from the wall where $c/C_{max} = 0{\cdot}5$

$$\lambda^+ = (a)^{2/(b+2)}\left[(\ln 2)\frac{(b+2)^2}{b}\right]^{b/(b+2)}\left(\frac{x^+}{N_{Sc,\,t}}\right)^{b/(b+2)} \tag{2.3}$$

(This is derived from equation (A.28) in [2]).

3. DETERMINATION OF THE PROPERTIES OF THE VELOCITY BOUNDARY LAYER

The theory of [2] is based, as already mentioned, on the familiar power-law velocity profile of the form

$$y^+ = a(u^+)^b \tag{3.1}$$

In [1], the experimental observations of velocity profiles are shown to give good agreement with such a power law when $b = 7$; it is clear, however, from the observations that $b = 6$ would fit the data just as well. We use $b = 7$ below.

The corresponding value of a was obtained as follows. From the integral momentum equation, combined with (3.1), we can derive:

$$\frac{\delta}{X'} = (a)^{2/(b+3)}\left[\frac{b}{(b+2)(b+3)}\right]^{-(b+1)/(b+3)}\left[\frac{U_{amb}X'}{\nu}\right]^{-2/(b+3)} \tag{3.2}$$

where δ is the thickness of the velocity boundary layer, and X' is the distance downstream from the origin of the velocity boundary layer. The experimental values of δ are given in [1], and the origin of the turbulent boundary layer can be assumed to be at the saw tooth (shown in Fig. 1 in [1]), that is at the station 5 ft 1 in. Corresponding values of δ/X' have therefore been plotted against

* The equation in [2] is in terms of temperature. The change from temperature to concentration has been made here in the conventional way.

$U_{amb}X'/\nu$ as shown in Fig. 1. It can be seen that though there is scatter, the points for $U_{amb} = 9$ and 12 ft/s satisfactorily define a single straight line of slope $-0{\cdot}2$, i.e. $-2/(b+3)$ with $b = 7$. The value of a which corresponds to this straight line, namely $a = 2{\cdot}08 \times 10^{-7}$, has been adopted for the following analysis, for all free stream velocities. (The values recommended in [2] are $a = 2{\cdot}412 \times 10^{-7}$, and $b = 7$).

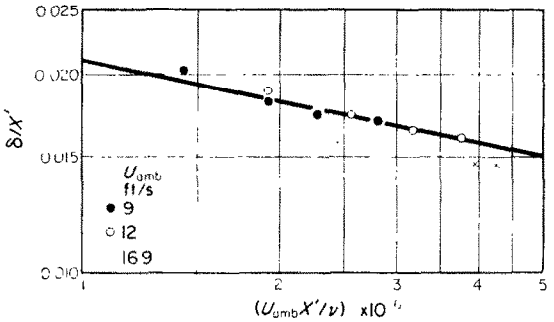

FIG. 1. Variation of the boundary-layer thickness.

4. COMPARISON WITH EXPERIMENT

4.1 *Concentration profiles*

As indicated earlier, the theory of [2] leads to the equation (2.1) which, for $b = 7$, takes the form

$$c/C_{max} = \exp\left[-0{\cdot}693(y/\lambda)^{9/7}\right] \qquad (4.1.1)$$

This equation is represented in Fig. 2 by the full curve. The experimental results of [1] for the intermediate zone are also shown on the same diagram. It is worth remarking here that, if the power of (y/λ) in the exponent were increased from 9/7, the theoretical curve would pass more centrally through the band of experimental points. Such a change would follow by decreasing b to 6, or even 5, in the velocity-profile power law, and as already pointed out, the experimental observations given in [1] justify a value of b less than 7.

4.2 *Concentration at the wall*

Equation (2.2) gives $(C_{max}\mu/G\rho)$ as a function of x^+. To draw this curve, it was necessary to choose a value of $N_{Sc,\,t}$, the turbulent Schmidt number. Since very few data are available to guide this choice, two different values were used, $N_{Sc,\,t} = 0{\cdot}9$ and $N_{Sc,\,t} = 0{\cdot}72$, the latter being the same as the laminar Schmidt number, as given in [1]. The two straight lines in Fig. 3 show the

$$(C_{max}\mu/G\rho) \sim x^+$$

relation as given by equation (2.2) for the two values of $N_{Sc,\,t}$.

As defined, in [2],

$$x^+ = \int_{X_o'}^{X'} (c_f/2)^{\frac{1}{2}}\, d(U_{amb}X'/\nu) \qquad (4.2.1)$$

where X'_o is the distance of the line source from the origin of the velocity boundary layer.

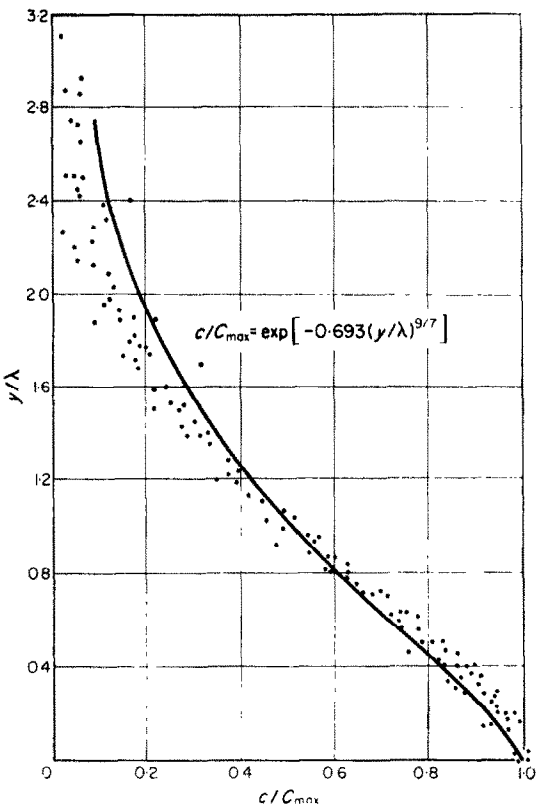

FIG. 2. Concentration profile.

As a result of the power-law representation of the velocity profile, we derive:

$$\frac{c_f}{2} = \left[\frac{ab}{(b+2)(b+3)}\right]^{2/(b+3)} \left[\frac{U_{amb}\,X'}{\nu}\right]^{-2/(b+3)} \qquad (4.2.2)$$

On substituting (4.2.2) into (4.2.1) we obtain:

$$x^+ = \left[\frac{ab}{(b+2)(b+3)}\right]^{1/(b+3)} \frac{(b+3)}{(2+b)} \left[\left(\frac{U_{amb}\,X'}{\nu}\right)^{(b+2)/(b+3)} - \left(\frac{U_{amb}\,X_o'}{\nu}\right)^{(b+2)/(b+3)}\right] \qquad (4.2.3)$$

The experimental points of Fig. 6 of [1] are presented in Fig. 3 of the present communication after making the change from x to x^+ by use of equation (4.2.3). It can be seen that the theoretical straight lines have the right slope, as defined by the experimental points, and that the line for $N_{Sc,\,t} = 0{\cdot}72$ is in better agreement with the experimental points.

4.3 *Distance, λ, from the wall where $c/C_{max} = 0{\cdot}5$*

Equation (2.3) gives λ^+ as a function of x^+. This is

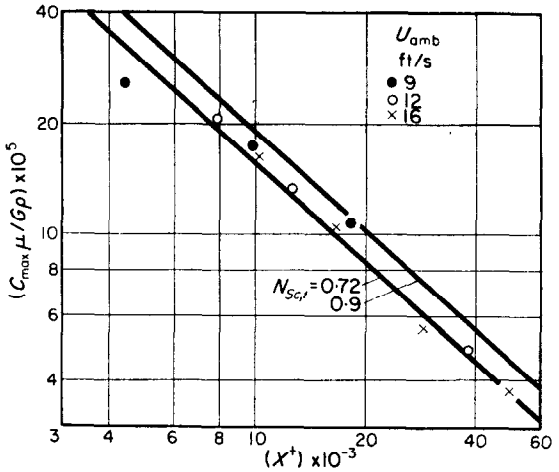

FIG. 3. Variation of the wall concentration.

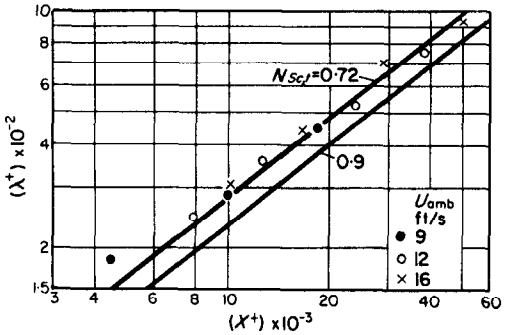

FIG. 4. Variation of λ^+ with x^+.

shown in Fig. 4 by two straight lines corresponding to the two values of $N_{Sc,\,t}$.

As defined in [2],

$$\lambda^+ = (c_f/2)^{\frac{1}{2}}\,(U_{amb}\,\lambda/\nu) \qquad (4.3.1)$$

On substituting (4.2.2) into (4.3.1) we find:

$$\lambda^+ = \frac{U_{amb}\,\lambda}{\nu}\left[\frac{ab}{(b+2)(b+3)}\right]^{1/(b+3)}\left[\frac{U_{amb}\,X'}{\nu}\right]^{-1/(b+3)} \qquad (4.3.2)$$

The experimental points of Fig. 6 of [1] are presented in Fig. 4 of the present communication, after transformation to the λ^+ and x^+ co-ordinates by use of equations (4.3.2) and (4.2.3). Here again, the agreement with the theory is quite good for $N_{Sc,\,t} = 0{\cdot}72$.

5. CONCLUSIONS

(1) The comparison with experiment displayed in Figs. 2–4, shows that the theory given by Spalding [2] is satisfactory for the diffusion of matter from a line source into an already developed turbulent boundary layer.

(2) When looking for the reasons why the agreement between the theory and the experimental results is not even better, it is important to recall the following points:

(i) The velocity profiles are described by a power law. Better expressions exist, but are more difficult to use. There is, also considerable latitude available in the choice of a and b in the power-law formula.

(ii) A single value of Schmidt number is used in the theoretical solution. In practice, some variation of Schmidt number across the boundary layer can be expected. Further, the evidence guiding the choice of this single value is very slight indeed.

(3) Figures 3 and 4 indicate that $N_{Sc,\,t} = 0{\cdot}72$ is a better value to choose than 0·9. However, because of the use of power law itself, and of the uncertainties in the values of a and b, this cannot be considered as a *determination* of the value of $N_{Sc,\,t}$.

REFERENCES

1. M. POREH and J. E. CERMAK, Study of diffusion from a line source in a turbulent boundary layer, *Int. J. Heat Mass Transfer* **7**, 1083–1095 (1964).
2. D. B. SPALDING, Contribution to the theory of heat transfer across a turbulent boundary layer, *Int. J. Heat Mass Transfer* **7**, 743–761 (1964).